J Mater Sci: Mater Electron (2017) 28:3774–3779
DOI 10.1007/s10854-016-5987-y

Simple synthesis and characterization of zinc manganite nanoparticles: investigation of surfactants effect and its photocatalyst application

Ruhollah Talebi[1]

Received: 5 August 2016 / Accepted: 31 October 2016 / Published online: 11 November 2016

Abstract In the current study, an attempt is made to synthesize and characterization of zinc manganite ($ZnMn_2O_4$) nanoparticles in an aqueous environment through the novel sol–gel method. Besides, three surfactants as polyvinylpyrrolidone, ethylene diamine tetraacetic acid, and sodium dodecyl sulfate were used to investigate their effects on the morphology and particle size of $ZnMn_2O_4$ nanoparticles. This method starts from of the precursor complex, and involves the formation of homogeneous solid intermediates, reducing atomic diffusion processes during thermal treatment. The formation of pure crystallized $ZnMn_2O_4$ nanocrystals occurred when the precursor was heat-treated at 800 °C in air for 300 min. $ZnMn_2O_4$ nanoparticles were characterized by UV–Vis diffuse reflectance spectroscopy, energy dispersive X-ray microanalysis, field emission scanning electron microscopy, and X-ray diffraction. The magnetic properties of as-prepared $ZnMn_2O_4$ nanoparticles were also investigated with vibrating sample magnetometer. Photocatalytic property of $ZnMn_2O_4$ nanoparticles was examined by degradation of methyl orange as organic pollutant in water under UV light irradiation.

1 Introduction

Materials at the nanometer scale have been studied for decades because of their unique properties arising from the large fraction of atoms residing on the surface, and also from the finite number of atoms in each crystalline core. Especially, because of the increasing need for high area density storage, the synthesis and characterization of semiconductor nanocrystals have been extensively investigated. In particular, nanosized semiconductor particles with suitable surface areas and a variety of morphologies offer great opportunity. Compared to other potential photocatalysts, iron oxides are plentiful in nature and environmentally benign [1–11]. Zinc manganite ($ZnMn_2O_4$) is one of the most attractive compounds of the AB_2O_4 series because of its low oxidation potential and low material cost [12]. The electrochemical properties of various $ZnMn_2O_4$ structures such as nanopowders, nanowires, hollow microspheres, and ball-in-ball microspheres have been investigated [13–17]. These nano-structured $ZnMn_2O_4$ materials have been prepared primarily by liquid solution methods such as sol–gel, coprecipitation, hydrothermal, and solvothermal processes. Manganese spinel ternary systems belong to a class of interesting and useful materials due to their unique electrical and magnetic properties. Spinel materials based on 3-D transition-metal oxides of Mn and Zn have been many investigations due to their outstanding semiconducting properties depending upon their applications concern mainly temperature sensing devices [18]. Generally, the manganites based on divalent metal oxides are referred to as negative temperature coefficient thermistors [19–21]. So, these materials can be used as temperature and heat sensors, fire detectors, power sensing terminations, temperature compen-sating attenuators, adsorbents, and catalysts [22–24] Zinc manganite, $ZnMn_2O_4$, is one of the important mixed transition-metal oxides due to its potential application. It was found that $ZnMn_2O_4$ was an efficient catalyst for the reduction of NO to N_2 by several types of hydrocarbons [25, 26]. Furthermore, to investigate the effect of different surfactants such as polyvinylpyrrolidone (PVP), ethylene diamine tetraacetic acid (EDTA), and sodium dodecyl sulfate (SDS) on

✉ Ruhollah Talebi
ruhollahtalebi90@gmail.com

[1] Young Researchers and Elite Club, Central Tehran Branch, Islamic Azad University, Tehran, Iran

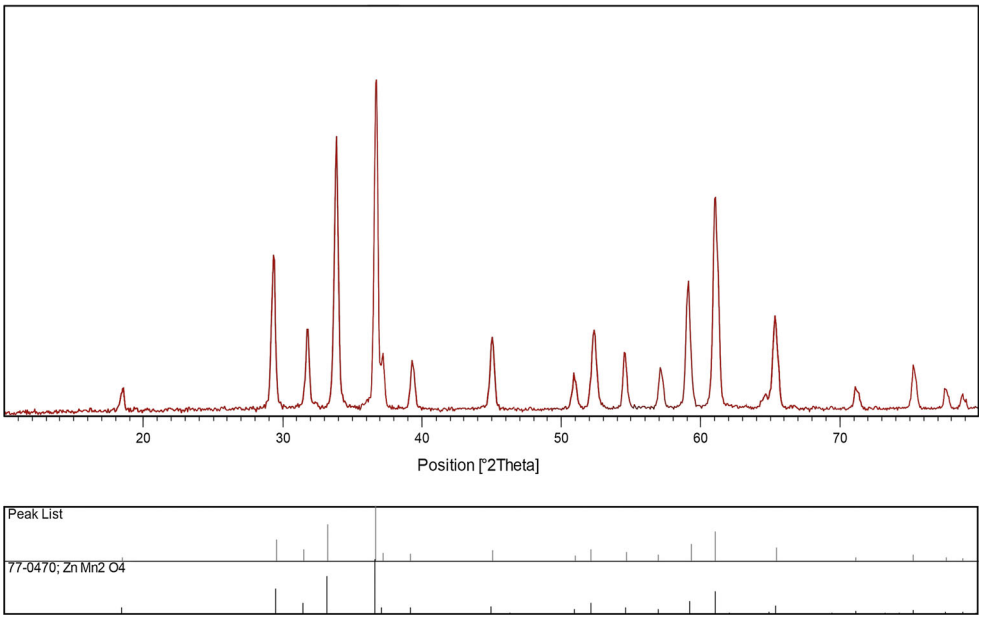

Fig. 1 XRD pattern of $ZnMn_2O_4$ nanoparticles calcined at 800 °C

the morphology, particle size, and crystal structure of the products several experiments were performed. To evaluate the catalytic properties of nanocrystalline $ZnMn_2O_4$, the photocatalytic degradation of methyl orange under UV light irradiation was carried out.

2 Experimental

2.1 Characterization

X-ray diffraction (XRD) patterns were recorded by a Philips-X'PertPro, X-ray diffractometer using Ni-filtered Cu Kα radiation at scan range of $10 < 2\theta < 80$. Scanning electron microscopy (SEM) images were obtained on LEO-1455VP equipped with an energy dispersive X-ray spectroscopy. Spectroscopy analysis (UV–Vis) was carried out using shimadzu UV–Vis scanning UV–Vis diffuse reflectance spectrometer. The energy dispersive spectrometry (EDS) analysis was studied by XL30, Philips microscope. The magnetic measurement of samples were carried out in a vibrating sample magnetometer (VSM) (Meghnatis Daghigh Kavir Co.; Kashan Kavir; Iran) at room temperature in an applied magnetic field sweeping between ±10,000 Oe.

2.2 Synthesis of $ZnMn_2O_4$ nanoparticles

All of the chemicals were used as received without further purifications. At first, 2 mmol of manganese nitrate, and of different surfactants were dissolved in 10 ml distilled in water and stirred for 15 min. Then, 1 mmol of zinc nitrate was added drop wise into solution. After wards, the final mixed solution was kept stirring to form a gel at 90 °C. Finally, the obtained product was placed in a conventional furnace in air atmosphere for 300 min and calcine at 800 °C. After thermal treatment, the system was allowed to cool to room temperature naturally, and the obtained precipitate was collected. Reaction conditions are listed in Table 1.

2.3 Photocatalysis experiments

The methyl orange (MO) photodegradation was examined as a model reaction to evaluate the photocatalytic activities of the $ZnMn_2O_4$ nanoparticles. The photocatalytic experiments were performed under an irradiation ultraviolet light. The photocatalytic activity of nanocrystalline zinc manganite obtained was studied by the degradation of methyl orange solution as a target pollutant. The photocatalytic degradation was performed with 50 ml solution of methyl orange (0.0005 g) containing 0.1 g of $ZnMn_2O_4$. This mixture was aerated for 30 min to reach adsorption equilibrium. Later, the mixture was placed inside the photoreactor in which the vessel was 15 cm away from the ultraviolet source of 400 W mercury lamps. The photocatalytic test was performed at room temperature. Aliquots of the mixture were taken at definite interval of times during the irradiation, and after centrifugation they were analyzed by a UV–Vis spectrometer. The methyl orange (MO) degradation percentage was calculated as:

$$\text{Degradation rate}\,(\%) = 100\,(A_0 - A_t)\,/\,A_0 \quad (1)$$

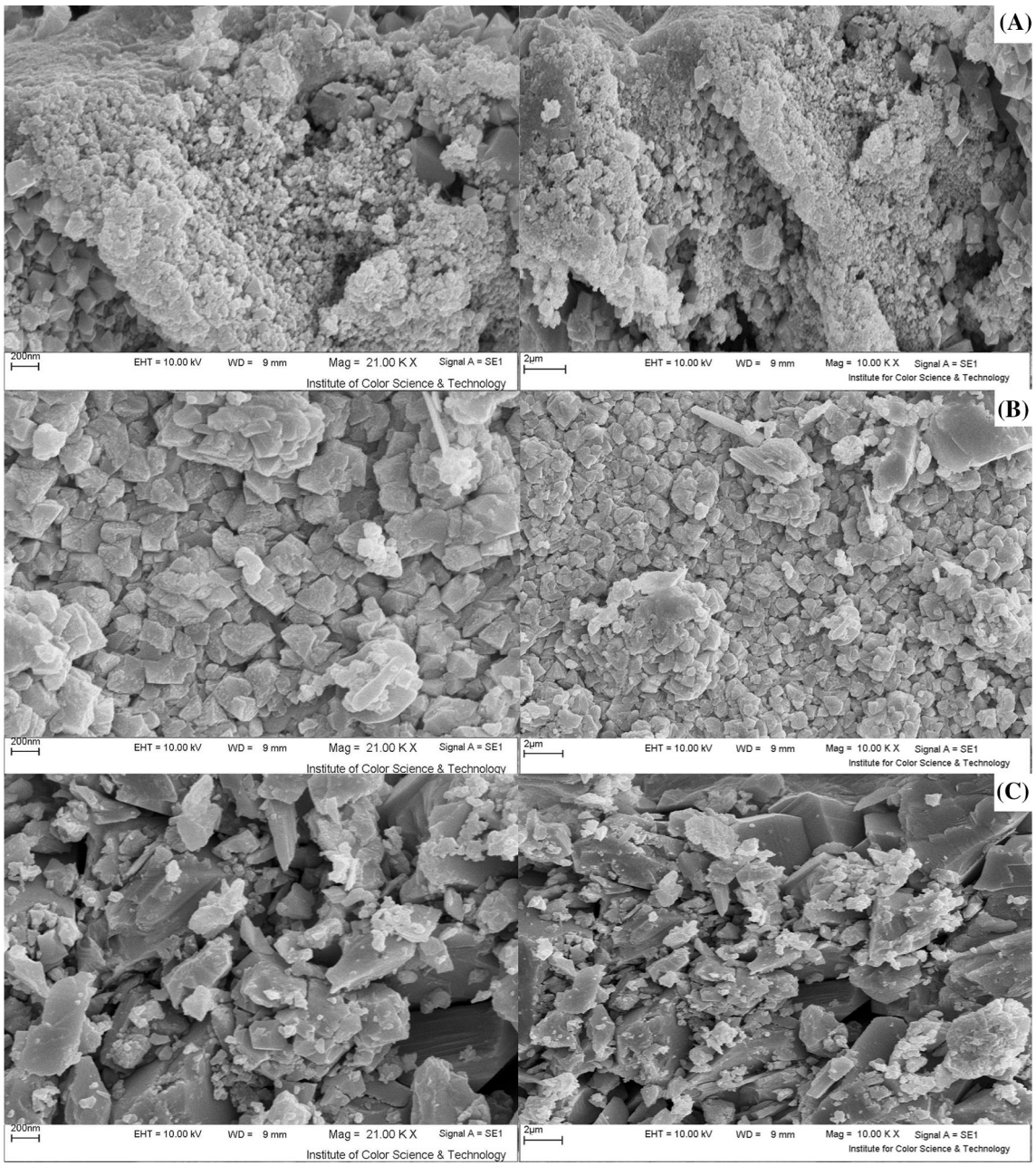

Fig. 2 SEM image of $ZnMn_2O_4$ nanoparticles calcined at 800 °C **a** sample 1 **b** sample 2 **c** sample 3

Where A_t and A_0 are the obtained absorbance value of the methyl orange solution at t and 0 min by a UV–Vis spectrometer, respectively.

3 Results and discussion

Figure 1 shows a typical XRD pattern ($10° < 2\theta < 80°$) of $ZnMn_2O_4$ nanoparticles. Based on the Fig. 1, the diffraction peaks can be indexed to pure tetragonal phase of $ZnMn_2O_4$ (space group of I41/amd and JCPDS No. 77-0470). No other crystalline phases were detected. From XRD data, the crystallite diameter (D_c) of $ZnMn_2O_4$ nanoparticles was calculated to be 12 nm using the Scherer equation:

$$D_c = K\lambda/\beta\cos\theta \quad \text{Scherer equation}$$

Where β is the breadth of the observed diffraction line at its half intensity maximum (400), K is the so-called shape factor, which usually takes a value of about 0.9, and λ is the wavelength of X-ray source used in XRD. In recent years, there has been considerable interest in control of

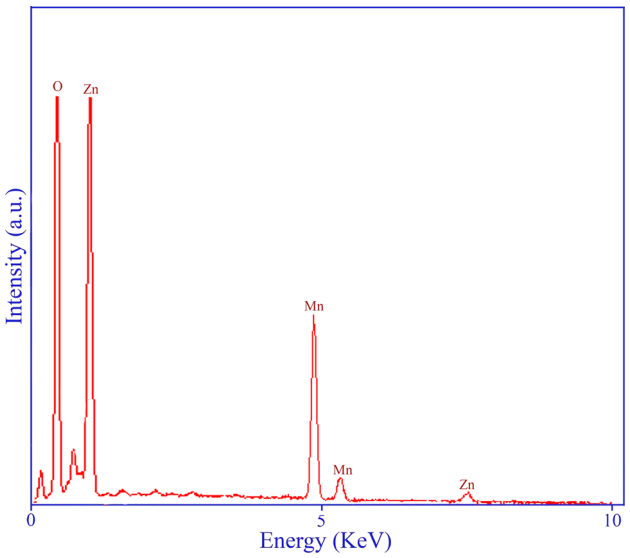

Fig. 3 EDS pattern of $ZnMn_2O_4$ nanoparticles calcined at 800 °C

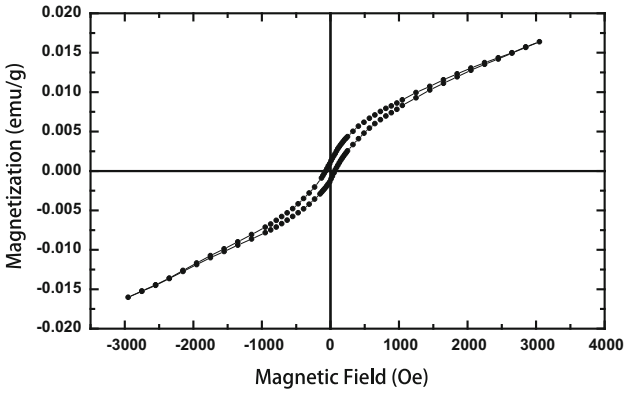

Fig. 4 VSM curves of $ZnMn_2O_4$ nanoparticles calcined at 800 °C

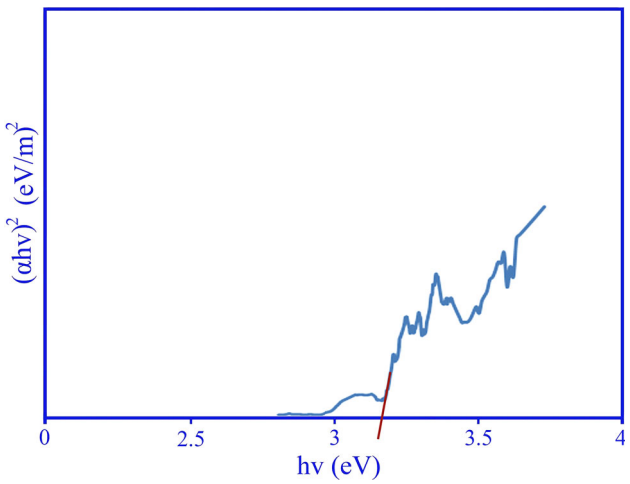

Fig. 5 DRS pattern of $ZnMn_2O_4$ nanoparticles calcined at 800 °C

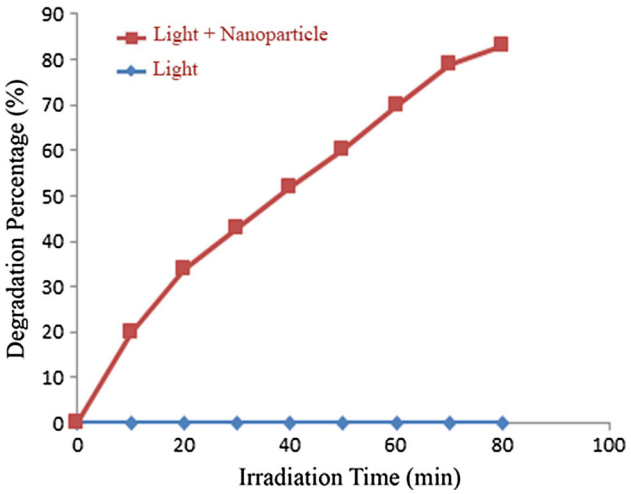

Fig. 6 Photocatalytic methyl orange degradation of $ZnMn_2O_4$ nanoparticles (sample 1) under ultraviolet light

Table 1 Reaction conditions for $ZnMn_2O_4$ nanoparticles

Sample No.	Surfactants	Temperature °C	Decolorization (%)
1	PVP	800	83
2	EDTA	800	–
3	SDS	800	–

shape and particle size of nanoparticles through the control of reaction parameters thanks to the fact that properties of nanoparticles are highly depend on their particle size and shape [21–33]; therefore, we performed several experiments to investigate the effect of different surfactants such as polyvinylpyrrolidone (PVP), ethylene diamine tetra-acetic acid (EDTA), and sodium dodecyl sulfate (SDS) on the morphology and particle size of the $ZnMn_2O_4$ nanoparticles. Figure 2a–c shows the SEM images of $ZnMn_2O_4$ nanoparticles in the presence of (PVP), (EDTA), and (SDS) as the surfactant accordance with sample 1–3, respectively. Based on the Fig. 2c, in the presence of SDS as the surfactant, products mainly consist of agglomeration nanoparticles. Furthermore, in the presence of PVP and EDTA as surfactant products have smaller size than SDS as the surfactant. The final products mainly consist of nanoparticles with average particle size 40–80 nm. Therefore, surfactants cause to increase the particle size of final products. The EDS analysis measurement was used to investigate the chemical composition and purity of $ZnMn_2O_4$ nanoparticles. According to the Fig. 3, the product consists of Zn, Mn, and O elements. Furthermore,

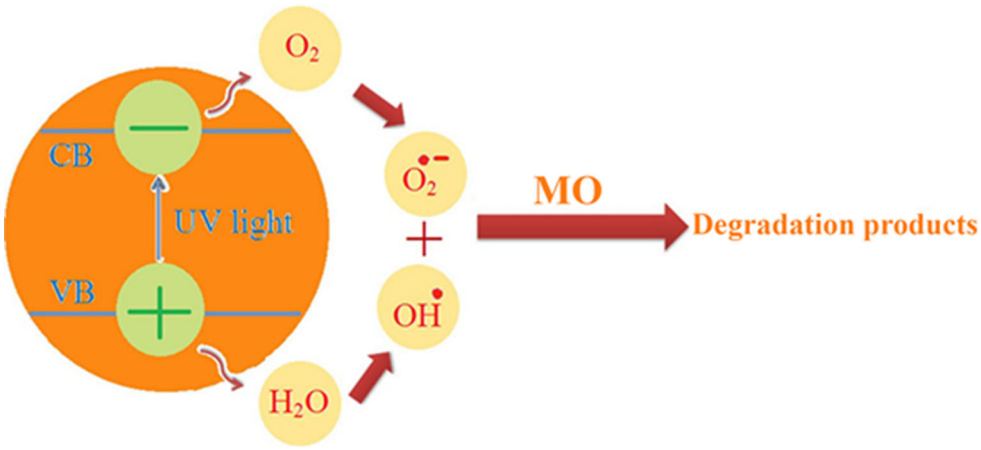

Scheme.1 Reaction mechanism of methyl orange photodegradation over $ZnMn_2O_4$ nanoparticles under UV light irradiation

neither N nor C signals were detected in the EDS spectrum, which means the product is pure and free of any surfactant or impurity. The hysteresis loop of $ZnMn_2O_4$ nanoparticles was studied to examine their magnetic properties (Fig. 4). At 300 K the remanent magnetization (Mr) is 0.002 emu/g, the coercive field (Hc) is 70 Oe and the magnetization at saturation (Ms) is estimated to be only 0.015 emu/g (the saturation magnetization Ms was determined from the extrapolation of curve of H/M versus H). To investigate the optical properties of the $ZnMn_2O_4$, UV–Vis spectrum was recorded. Figure 5 shows the UV–Vis diffuse reflectance spectrum of $ZnMn_2O_4$ nanoparticles. Using Tauc's formula, the band gap can be obtained from the absorption data. The energy gap (Eg) of the nanocrystalline $ZnMn_2O_4$ has been estimated by extrapolating the linear portion of the plot of $(\alpha h\nu)^2$ against $h\nu$ to the energy axis. The Eg value of the nanocrystalline $ZnMn_2O_4$ calculated to be 3.2 eV. According to the obtained Eg value, as-prepared nanoparticles $ZnMn_2O_4$ sample can be employed as the photocatalyst. Photodegradation of methyl orange as water contaminant under UV light illumination was employed to evaluate the properties of the as-synthesized $ZnMn_2O_4$ nanoparticles. Figure 6 exhibits the obtained result. No methyl orange was practically broken down after 80 min without employing UV light illumination or as-prepared $ZnMn_2O_4$ nanoparticles. This observation illustrated that the contribution of self-degradation was insignificant. The proposed mechanism of the photocatalytic degradation of the methyl orange can be assumed as:

$$ZnMn_2O_4 + h\nu \rightarrow ZnMn_2O_4^{\cdot} + e^- + h^+ \quad (2)$$

$$h^+ + H_2O \rightarrow OH^{\cdot} \quad (3)$$

$$e^- + O_2 \rightarrow O_2^{\cdot -} \quad (4)$$

$$OH^{\cdot} + O_2^{\cdot -} + \text{methyl orange} \rightarrow \text{degradation products} \quad (5)$$

Utilizing photocatalytic calculations by Eq. (1), the methyl orange degradation was about 83% after 80 min illumination of UV light. This obtained result demonstrates that as-prepared $ZnMn_2O_4$ nanoparticles have high potential to be applied as favorable and appropriate material for photocatalytic applications under illumination of UV light. The heterogeneous photocatalytic processes have diffusion, adsorption and reaction steps. It has been shown that the desirable distribution of the pore has effective and important impact on the diffusion of thereactants and products, and therefore effects on the photocatalytic activity. It seems that the enhanced photocatalytic activity of the as-obtained nanoparticles $ZnMn_2O_4$ can be owing to desirable and appropriate distribution of the pore, high hydroxyl amount and high separation rate of charge carriers (Scheme 1). Furthermore, this route is facile to operate and very suitable for industrial production of $ZnMn_2O_4$ nanoparticles.

4 Conclusions

In summary, $ZnMn_2O_4$ nanoparticles have been successfully prepared by using manganese nitrate and zinc nitrate via a sol–gel method at 800 °C for 5 h. The final products were analyzed by SEM, EDS, VSM, EDS and XRD. The XRD results indicated that pure phase of $ZnMn_2O_4$ could be obtained by this method. VSM analyzes indicates a ferromagnetic behavior for the synthesized nanoparticles. When as prepared nanocrystalline $ZnMn_2O_4$ was utilized as photocatalyst, the percentage of methyl orange degradation was about 83% after 80 min irradiation of UV light. This result suggests that as-obtained nanocrystalline $ZnMn_2O_4$ as favorable material has high potential to be used for photocatalytic applications under UV light.

Acknowledgements Authors are grateful to council of University of Central Tehran for providing financial support to undertake this work.

References

1. S. Khademolhoseini, M. Zakeri, S. Rahnamaeiyan, M. Nasiri, R. Talebi, J. Mater. Sci. Mater. Electron. **26**, 7303 (2015)
2. R. Talebi, S. Khademolhoseini, S. Rahnamaeiyan, J. Mater. Sci. Mater. Electron. **27**, 1427 (2016)
3. S. Khademolhoseini, R. Talebi, J. Mater. Sci. Mater. Electron. **27**, 2938 (2016)
4. S.S. Hosseinpour-Mashkani, S.S. Hosseinpour-Mashkani, A. Sobhani-Nasab, J. Mater. Sci. Mater. Electron. **27**, 4351 (2016)
5. M. Panahi-Kalamuei, M. Mousavi-Kamazani, M. Salavati-Niasari, J. Nanostruct. **4**, 459 (2014)
6. A. Esmaeili-Bafghi-Karimabad, D. Ghanbari, M. Salavati-Niasari, H. Safardoust-Hojaghan, J. Nanostruct. **5**, 263 (2015)
7. M. Ebadi, H. Shagholani, H. Jahangir, J. Nanostruct. **6**, 23 (2016)
8. L. Nejati-Moghadam, A. Esmaeili Bafghi-Karimabad, M. Salavati-Niasari, H. Safardoust, J. Nanostruct. **5**, 47 (2015)
9. M. Rahimi-Nasarabadi, J. Nanostruct. **4**, 211 (2014)
10. A. Sobhani-Nasab, M. Sadeghi, J. Mater. Sci. Mater. Electron. **27**, 7933 (2016)
11. S. Moshtaghi, D. Ghanbari, M. Salavati-Niasari, J. Nanostruct. **5**, 169 (2015)
12. F.M. Courtel, H. Duncan, Y. Abu-Lebdeh, I.J. Davidson, J. Mater. Chem. **21**, 10206 (2011)
13. S.W. Kim, H.W. Lee, P. Muralidharan, D.H. Seo, W.S. Yoon, D.K. Kim, K.S. Kang, Nano Res. **4**, 505 (2011)
14. G.Q. Zhang, L. Yu, H.B. Wu, H.E. Hoster, X.W. Lou, Adv. Mater. **4**, 4609 (2012)
15. L.F. Xiao, Y.Y. Yang, J. Yin, Q. Li, L.Z. Zhang, J. Power Sources **194**, 1089 (2009)
16. Y.F. Deng, S.D. Tang, Q.M. Zhang, Z.C. Shi, L.T. Zhang, S.Z. Zhana, G.H. Chen, J. Mater. Chem. **21**, 11987 (2011)
17. L. Zhou, H.B. Wu, T. Zhu, X.W. Lou, J. Mater. Chem. **22**, 827 (2012)
18. S. Guillemet-Fritsch, C. Chanel, J. Sarrias, S.S. Bayonne, A. Rousset, X. Alcobe, Solid State Ion. **128**, 233 (2000)
19. G.D.C. de Györgyfalva, I.M. Reaney, J. Mater. Res. **18**, 1301 (2003)
20. R. Schmidt, A. Stiegelschmitt, A. Roosen, A.W. Brinkman, J. Eur. Ceram. Soc. **23**, 1549 (2003)
21. B. Viswanathan, V.R.K. Murthy, *Ferrite Materials Science and Technology*, 1st edn. (Toppan Company(s) Pte. Ltd., Singapore, 1990), pp. 2–16
22. V.I. Zaharov, A.O. Olesk, Elektronn. Teh. Ser Radiodetali i Kompon. **65**, 30 (1989)
23. V.I. Zaharov, A.O.A.O. Olesk, Zarub. Elektronn. Teh. **5**, 43 (1983)
24. J. Zhong, H.H. Bau, Am. Ceram. Soc. Bull. **80**, 39 (2001)
25. G. Ferraris, G. Fierro, M.L. Jacono, M. Inversi, Appl. Catal. B Environ. **36**, 251 (2000)
26. G. Ferraris, M.L. Jacono, R. Dragone, G. Ferraris, B. Andreozzi, G. Graziani, Appl. Catal. B Environ. **57**, 153 (2005)
27. A. Sobhani-Nasab, M. Behpour, J. Mater. Sci. Mater. Electron. **27**, 1191 (2016)
28. M. Maddahfar, M. Ramezani, M. Sadeghi, A. Sobhani-Nasab, J. Mater. Sci. Mater. Electron. **26**, 7745 (2015)
29. M.P. Mazhari, A. Abbasi, A. Derakhshan, M. Ahmadi J. Nanostruct. **1**, 99 (2016)
30. R. Talebi, J. Mater. Sci.: Mater. Electron. **6**, 5665 (2016)
31. E. Khosravifard, M. Salavati-Niasari, M. Dadkhah, G. Sodeifian, J. Nanostruct. **2**, 191 (2012)
32. M. Behpour, S.M. Ghoreishi, M. Salavati-Niasari, N. Mohammadi, J. Nanostruct. **2**, 317 (2012)
33. L. Hashemi, A. Tahmasian, A. Morsali, J. Abedini, J. Nanostruct. **2**, 163 (2012)